AD-A156 559   AN ACTIVE TRACKING BAND-PASS FILTER(U) DEFENCE RESEARCH   1/1
               ESTABLISHMENT VALCARTIER (QUEBEC) A MORIN ET AL.
               MAY 85 DREV-4347/85

UNCLASSIFIED   F/G 9/5   NL

NATIONAL BUREAU OF STANDARDS
MICROCOPY RESOLUTION TEST CHART

National Défense
Defence nationale

DREV REPORT 4347/85
FILE: 3621J-005
MAY 1985

CRDV RAPPORT 4347/85
DOSSIER: 3621J-005
MAI 1985

AN ACTIVE TRACKING BAND-PASS FILTER

A. Morin

P. Labbé

Centre de Recherches pour la Défense

Defence Research Establishment

Valcartier, Québec

BUREAU - RECHERCHE ET DÉVELOPPEMENT
MINISTÈRE DE LA DÉFENSE NATIONALE
CANADA

RESEARCH AND DEVELOPMENT BRANCH
DEPARTMENT OF NATIONAL DEFENCE
CANADA

85 06 25 304

Canada

AN ACTIVE TRACKING BAND-PASS FILTER

by

A. Morin and P. Labbé

CENTRE DE RECHERCHES POUR LA DEFENSE

DEFENCE RESEARCH ESTABLISHMENT

VALCARTIER

Tel: (418) 844-4271

Québec, Canada   May/mai 1985

SANS CLASSIFICATION

ABSTRACT

A frequency-agile tracking filter, which operates over a wide
frequency range with a high immunity to noise and interference, has been
designed. It consists of a second-order band-pass filter which is con-
tinuously tunable over the 5- to 140-kHz band. The resonant frequency
of the filter is adjusted by means of a feedback loop to the frequency
component of greatest amplitude in the input signal. The loop includes
a fast AGC amplifier, a fast frequency-to-voltage converter and a low-
pass filter. The components of the tracking filter are described and
analyzed. Analysis of the tracking filter, as regards its immunity to
noise and interference, its frequency agility and the stability of its
control loop, is also presented to optimize system parameters. Finally,
the performance of the processor is shown by experimental measurements.

RÉSUMÉ

On a conçu un filtre de poursuite agile en fréquence qui fonc-
tionne dans une large bande de fréquences tout en résistant au bruit et
aux interférences. Il comprend un filtre passe-bande du deuxième ordre
qui est constamment accordable dans la bande de 5 à 140 kHz. Une boucle
d'asservissement permet d'ajuster la fréquence du filtre à celle de la
composante de fréquence ayant l'amplitude la plus élevée dans le signal
d'entrée. Cette boucle comporte un amplificateur à commande automatique
de gain et un convertisseur de fréquence à tension rapides ainsi qu'un
filtre passe-bas. Tous les composants du filtre de poursuite sont
décrits et analysés. On a aussi procédé à l'analyse du filtre de pour-
suite, en ce qui concerne son agilité en fréquence, sa résistance au
bruit et aux interférences et la stabilité de sa boucle d'asservisse-
ment, en vue d'optimiser les paramètres du système. Finalement, la
performance du filtre est démontrée par des résultats expérimentaux.

A-1

TABLE OF CONTENTS

1.0 INTRODUCTION

This document describes a very frequency-agile tracking filter
which can be operated over a wide frequency range (5-140 kHz) with a
high immunity to noise and interferences. Tracking filters are narrow-
band filters which track wandering carrier frequencies. Their operation
is analogous to that of phase-locked loops except that these filters
preserve the amplitude of their input signals as well as their
frequencies.

In some approaches (Refs. 1, 2), the resonant frequency of a
tunable filter adjusts itself to coincide with the input frequency by
comparing the relative phase shift between the input and the output of
this filter. Examination of the performance achieved by these systems
reveals that they were unable to track in the 5- to 140-kHz band a
Doppler signal whose frequency and amplitude can shift rapidly and
greatly. This signal is mixed with noise and strong interferences.
Realized in a compact system, our concept gives a better performance as
regards the frequency-tracking range, the immunity to noise and
interference and the frequency agility so that it can process such a
Doppler signal. Basically, it consists of a second-order band-pass
filter which is characterized by a sharp and constant frequency-to-
bandwidth ratio. In closed loop, it operates like a very fast
discriminator over the 5- to 140-kHz band. It is continuously tunable
over that band by means of a feedback loop that senses its output and
adjusts its center frequency so as to keep the pass-band coincident with
the component of greatest amplitude in the input signal. The loop
includes a fast automatic gain control (AGC) amplifier which matches the
output of the band-pass filter to the input of a fast frequency-to-
voltage (F/V) converter. The loop allows the frequency-tracking filter
to remain locked on to the selected frequency even if it is varied
rapidly.

The components of the tracking filter are described and analyzed. Two models of tunable filters have been considered. The first concept has been realized by using multipliers as variable resistances which, in effect, vary the resonant frequency as the control voltage from the feedback loop is adjusted. The second version is quite similar to the first one except that the multipliers are substituted by operational transconductance amplifiers (OTAs).

The AGC amplifier was designed to get a short time constant and a wide-amplitude dynamic range while the F/V converter provides a short time constant as well as a low-voltage ripple at its output. These conditions control the loop speed that has to be as fast as the rate of change in frequency and amplitude of the signal to be tracked.

Analysis of the tracking filter regarding the immunity to noise and interference, the frequency agility and the stability of the control loop is also presented to determine the optimum setting of parameters such as the quality factor of the band-pass filter and the time constants of the AGC amplifier and F/V converter. Finally, from experimental results we can determine the performance of the tracking filter. In one laboratory test, the filter input is fed by the output of a programmable generator to determine its dynamic range, its frequency agility and its immunity to noise and interference. In another test, the filter is driven by a Doppler signal in the 5- to 140-kHz frequency band where the information to be detected is disturbed by strong interference.

This work was performed at DREV between September 1982 and April 1983 under PCN 21J05, Guidance and Control Concepts.

2.0 ANALYSIS OF THE FREQUENCY-TRACKING FILTER

The design of the tracking filter aims at providing frequency
agility and immunity to noise and interference over a wide frequency
range. Analysis of these properties is presented in this chapter to
assess the significance of the system parameters. In the first step, it
consists in finding the response of the processor when the signal to be
tracked is mixed with sources of interference. This procedure allows us
to set some characteristics of the band-pass filter, AGC amplifier and
F/V converter. In addition, the transfer function of the
frequency-tracking loop is given and the effects of the tuning errors
are evaluated. In another step, a frequency-modulated signal is used to
analyze the frequency agility of the filter.

2.1 Capability of Tracking a Frequency in the Presence of Interference

To analyze the capability of the system to track a frequency in
the presence of interference, let the input of the tracking filter
(Fig. 1) be driven by a signal constituted of N amplitudes and
frequencies. This signal is related as

$$v(t) = \sum_{i=1}^{N} A_i \cos(\omega_i t) \qquad [1]$$

The signal, after being processed by the second-order band-pass
filter initially tuned at a resonant frequency ω_o within the
bandwidth of the system, becomes

$$v_{BP}(t) = \sum_{i=1}^{N} V_i \cos(\omega_i t + \phi_i) \qquad [2]$$

where V_i is the amplitude of the signal at the frequency f_i seen at the output of the band-pass filter. If Q and K_F are defined as the quality factor and the gain of the filter respectively, this yields

$$V_i = \frac{A_i \; K_F \; \omega_i \; \omega_o}{\sqrt{\omega_o^2 \omega_i^2 + Q^2 (\omega_o^2 - \omega_i^2)^2}} \qquad [3]$$

$$\phi_i = \frac{\Pi}{2} - \arctan \frac{\omega_o \; \omega_i}{Q(\omega_o^2 - \omega_i^2)} \qquad [4]$$

```
                           ● OUTPUT
                         │
        ┌──────────────┐ │   ┌──────────────┐
 INPUT  │ SECOND-ORDER │ │   │     AGC      │
 ●───►  │ BAND-PASS    │─┼──►│  AMPLIFIER   │──────►──────┐
        │ FILTER       │ │   │              │            │
        └──────────────┘     └──────────────┘            │
             │   f_0                                      │
             │                                            │
             ▲                                            │
             │   ┌──────────────┐   ┌─────────────────┐   │
             │   │  LOW-PASS    │   │ FREQUENCY-TO-   │   │
             └───│  FILTER      │◄──│ VOLTAGE         │◄──┘
                 │              │   │ CONVERTER       │
                 └──────────────┘   └─────────────────┘
               │
               ● CONTROL VOLTAGE OF
                 THE BAND-PASS FILTER
```
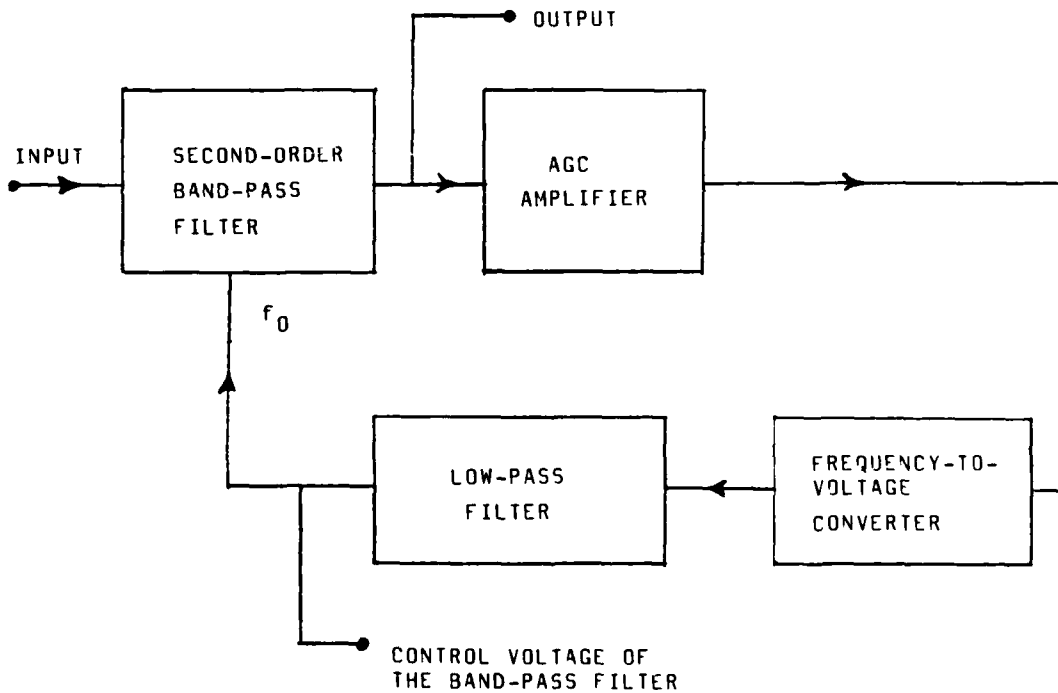
FIGURE 1 - Schematic of the frequency-tracking filter

The signal $v_{BP}(t)$ can be presented as an amplitude-modulated signal. Its carrier frequency identified by f_j is the frequency which has the greatest amplitude. If the phases ϕ_i are neglected, eq. 2 can be rewritten as

$$v_{BP}(t) = \cos \omega_j t (V_j + \sum_{i=1}^{N} V_i \cos(\omega_j - \omega_i)t) + \sin \omega_j t (\sum_{i=1}^{N} V_i \sin(\omega_j - \omega_i)t) \qquad [5]$$

for $i \neq j$.

The AGC amplifier detects both the amplitude of the carrier V_j and its amplitude modulation, processes this information by using a low-pass filter and finally, modifies its gain by means of a feedback network in an attempt to maintain the output at a constant voltage reference V_R. If the low-pass filter of the AGC amplifier is approximated by a first-order function whose pole frequency is located at ω_p, the gain of the amplifier can be presented as

$$k_{AGC}(t) = V_R \left\{ \left[V_j + \sum_{i=1}^{N} \frac{V_i \cos(\omega_j - \omega_i)t}{(1+(\frac{\omega_j - \omega_i}{\omega_p})^2)^{\frac{1}{2}}} \right]^2 + \left[\sum_{i=1}^{N} \frac{V_i \sin(\omega_j - \omega_i)t}{(1+(\frac{\omega_j - \omega_i}{\omega_p})^2)^{\frac{1}{2}}} \right]^2 \right\}^{-\frac{1}{2}} \qquad [6]$$

The signal at the output of the AGC amplifier v_A becomes

$$v_A(t) = k_{AGC}(t) \sum_{i=1}^{N} V_i \cos(\omega_i t + \phi_i) \qquad [7]$$

Equation 6 shows that, if the time constant of the AGC amplifier ($\tau_{AGC} = 1/\omega_p$) is great compared with the frequency difference $\omega_j - \omega_i$, the gain of the amplifier becomes simply V_R/V_j. In this situation, the amplifier will normalize the amplitude of the carrier and will amplify its modulation. If the time constant is kept small, the gain of the AGC amplifier is continuously modified to attenuate or eliminate the amplitude modulation.

The F/V converter is built to detect the carrier frequency of the signal described in eq. 5 which is the one characterized by the signal of greatest amplitude at the output of the AGC amplifier. The F/V output feeds a low-pass filter whose gain is adjusted to tune the resonant frequency of the band-pass filter.

The transfer function between the input frequency ω_j and the control voltage V_c is described by the relation

$$\frac{V_c(s)}{\omega_j(s)} = \left[\frac{V_c(s)}{V_L(s)}\right] \cdot \left[\frac{V_L(s)}{\omega_j(s)}\right] = \left[\frac{K_2}{\tau_3 s+1}\right] \cdot \left[\frac{K_3}{\tau_4 s+1}\right] \qquad [8]$$

where V_c = the control voltage which tunes the resonant frequency of the band-pass filter,

ω_j = the frequency of the signal of greatest amplitude at the output of the band-pass filter,

V_L = the voltage output of the F/V converter,

K_2 = the F/V gain factor,

K_3 = the gain of the low-pass filter,

τ_3 = the time constant of the F/V converter, and

τ_4 = the time constant of the low-pass filter.

Then, the resonant frequency of the band-pass filter will be tuned by the following command:

$$\omega_R(s) = \epsilon_1(s) + K_5\left[V_c(s) + \frac{K_3(RI(s) + V_E(s))}{\tau_4 s+1}\right] \qquad [9]$$

where K_5 is given in rad/s/V and must be equal to $1/K_2 K_3$; RI is the ripple voltage at the output of the F/V converter and V_E is the voltage error due to the nonlinearity of the ratio V_L/ω_j and to the variation of its gain K_2 with respect to temperature. The ratio of the control voltage of the band-pass filter to the resonant frequency is not necessarily linear and this generates the tuning error ϵ_1.

We deduce from eqs. 2 and 3 that the value of the quality factor
Q (frequency-to-bandwidth ratio) of the filter determines the immunity
of the system to noise and interference. A constant value of the Q
parameter insures a proportional rejection of the interference for all
frequencies within the tracking range of the filter. The time constant
of the AGC amplifier determines the maximum rate with which a variation
in the amplitude of the input signal can be followed by the processor.
As it is demonstrated by eqs. 6 and 7, an AGC amplifier characterized by
a short time constant advantages the frequency which has the greatest
amplitude.

Since the system does not use the feedback loop to correct the
error between the resonant frequency of the band-pass filter ω_R and
the frequency at the input of the F/V converter ω_j, the matching of
ω_R with ω_j in eq. 9 requires that the ratio V_L/ω_j of the F/V converter
and the ratio ω_R/V_c of the band-pass filter must be highly linear.

In addition, the speed of the frequency-tracking loop must be
limited because the ripple of the control voltage V_c depends on the
time constants τ_2 and τ_3. A tuning error will create an amplitude of
the frequency to be tracked. This attenuation, which increases with the
quality factor Q, diminishes the amplitude dynamic range of the
processor and its immunity to noise and interference.

2.2 Analysis of the Frequency Agility

To analyze the capability of the tracking filter to follow a
signal that varies in frequency, let the input of the tracking filter be
driven by a frequency-modulated signal $v_1(t) = \cos(\omega_c t + (\Delta f/f_m) \sin\omega_m t)$.
The signal that commands the resonant frequency of the band-pass filter

will be attenuated and phase-shifted by the F/V converter. From eqs. 8 and 9, it is written as

$$\omega_R(t) = \omega_c + \frac{2\pi\Delta f \cos\left(\omega_m t - \arctan\left\{(\tau_3 + \tau_4)\,\omega_m/1 - \tau_3\tau_4\omega_m^2\right\}\right)}{\sqrt{(1 - \tau_3\tau_4\omega_m^2)^2 + (\tau_3 + \tau_4)^2\,\omega_m^2}} \quad [10]$$

if we assume that the voltage errors ε_1, V_E and RI in eq. 9 are negligible. The output signal of the band-pass filter is found by substituting eq. 10 in the transfer function of the band-pass filter. This gives

$$v_{BP}(t) = \frac{\frac{\omega_R(t)}{Q}(\omega_c + 2\pi\Delta f\cos\omega_m t)\cos\left(\omega_c t + \frac{\Delta f \sin\omega_m t}{f_m} + \phi_1\right)}{\left\{\left[\frac{\omega_R(t)}{Q}(\omega_c + 2\pi\Delta f\cos\omega_m t)\right]^2 + \left[\omega_R^2(t) - (\omega_c + 2\pi\Delta f\cos\omega_m t)^2\right]^2\right\}^{\frac{1}{2}}} \quad [11]$$

where $\phi_1 = \frac{\pi}{2} - \arctan \dfrac{\omega_R^2(t) - (\omega_c + 2\pi\Delta f\cos\omega_m t)^2}{\frac{\omega_R(t)}{Q}(\omega_c + 2\pi\Delta f\cos\omega_m t)}$.

Examination of eq. 11 reveals that the output signal of the band-pass filter simultaneously becomes modulated in amplitude and in frequency. The amplitude modulation, whose frequency is twice greater than the modulation frequency f_m of the input signal, increases with the index of the frequency modulation $(\Delta f/f_m)$, the quality factor of the band-pass filter and the response time of the F/V converter. To allow the processor to be frequency locked on to the input signal, the modulation frequency (f_m) of this signal must be smaller than $1/2\tau_{AGC}$ and the magnitude of the amplitude modulation of the signal $v_{BP}(t)$ must be smaller than the dynamic amplitude range of the AGC amplifier. Thus, the frequency agility of the processor depends also on the performance of the AGC amplifier.
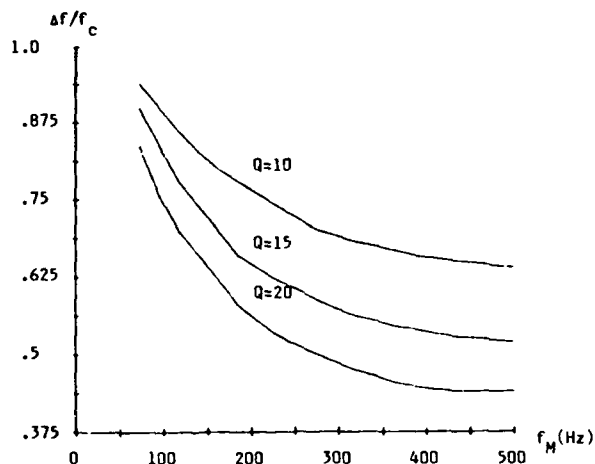
FIGURE 2 - Maximum values of the ratio $\Delta f/f_c$ (frequency deviation to carrier frequency) as functions of the frequency of the modulating input signal for three values of the quality factor Q (10, 15 and 20). The frequency-tracking loop of the processor has a time constant of 650 µs while the AGC amplifier has a time constant of 1 ms and an amplitude dynamic range of 60 dB.

Figure 2 illustrates the behavior of the tracking filter when the time constants τ_3 and τ_4 have been set to 220 and 270 µs yielding a frequency-tracking loop with a time constant of approximately 650 µs. In addition, we assume that the AGC amplifier is characterized by a time constant of 1 ms and an amplitude dynamic range of 50 dB. The signal $v_{BP}(t)$ described in eq. 11 has been computed and the values of the ratio $\Delta f/f_c$ that produce amplitude variations of $v_{BP}(t)$ equal to 60 dB have been plotted as a function of the frequency of the modulating signal for the following values of the quality factor Q, i.e. 10, 15 and 20. For any value of f_c and f_m, these curves give the maximum frequency deviation (Δf) which can be substituted for the input modulating signal to maintain the tracking filter frequency locked. It is shown that the curves are shifted down when the quality factor Q increases. Thus, the higher the frequency agility of the processor, the more its immunity to noise and interferences must be diminished. The value of f_m is limited to 500 Hz, which is equal to $1/2\tau_{AGC}$. In Fig. 2, the amplitude of the input signal of the tracking filter is assumed to be set to the

maximum value that can be injected without saturation of the AGC amplifier ($E_i = E_{max}$). This allows the tracking filter to use the full dynamic range of the AGC amplifier to track the signal in frequency. However, if a signal with a lower amplitude is injected ($E_i < E_{max}$), the effective dynamic range of the AGC amplifier to track this signal is decreased by the amplitude ratio E_i/E_{max}.

3.0 REALIZATION OF THE FREQUENCY-TRACKING FILTER

The frequency-tracking filter is composed of a tunable second-order filter which must provide the following properties in the range of 5-140 kHz :

(1) a constant Q,

(2) a constant resonant-frequency gain, and

(3) a resonant frequency proportional to the control voltage.

Two models that are derived from the biquad structure can meet these requirements. The first configuration is built with analog multipliers and the other one uses OTAs.

The frequency-tracking loop senses the output of the band-pass filter E_o and produces the control voltage that moves the resonant frequency f_R of the filter towards the frequency that dominates E_o (this frequency is identified by f_A). When f_A varies, the loop readjusts f_R to track f_A. If the amplitude of a signal at frequency f_B (different from f_A) becomes superior to that of the signal corresponding to f_A at the output of the band-pass, then f_R will be moved to f_B and f_B will replace f_A. The system centered on f_A attenuates the noise and interference (located outside its frequency

bandwidth) that disturb the detection of f_A. In addition, the frequency-tracking loop must be fast enough to lock on to f_A when it is varying at high rates.

This loop is composed of an AGC amplifier, an F/V converter and a low-pass filter. Let us analyze each of these units.

3.1 Tunable Band-Pass Filter with Multipliers

A voltage-tunable active filter can be created by adding two multipliers to a universal active filter. The resonant frequency of this filter varies linearly with the control voltage and it simultaneously provides low-pass, high-pass and band-pass outputs. Ideally, the filter Q factor and pass-band gain remain constant while the frequency is varied. The voltage transfer function between the band-pass output and the input is related as follows :

$$\frac{E_o(s)}{E_1(s)} = \frac{K_F(\omega_o/Q)s}{s^2 + (\omega_o/Q)\ s + \omega_o^2} \qquad [12]$$

where $e_o(t)$ = the output signal of the band-pass filter, whose Laplace transform is noted by $E_o(s)$,

$e_i(t)$ = the input signal of the band-pass filter, whose Laplace transform is noted by $E_i(s)$,

K_F = the gain of the filter,

f_o = the resonant frequency,

s = the Laplace operator, and

Q = quality factor of the filter defined as the ratio of the frequency f_o to the bandwidth of the filter.

If we suppose that the operational amplifiers and the multipliers are ideal components, the circuit of Fig. 3 is defined as follows (Ref. 3) :

$$[f_o]_{max} = \frac{1}{2\pi} \left(\frac{K_X}{R_1 R_2 C_1 C_2}\right)^{\frac{1}{2}} \qquad [13]$$

$$Q = \text{quality factor} = \frac{1 + K_Y}{1 + K_X} \left(\frac{K_X R_1 C_1}{R_2 C_2}\right)^{\frac{1}{2}} \qquad [14]$$

$$K_F = \text{gain of the filter} = -K_Y \qquad [15]$$
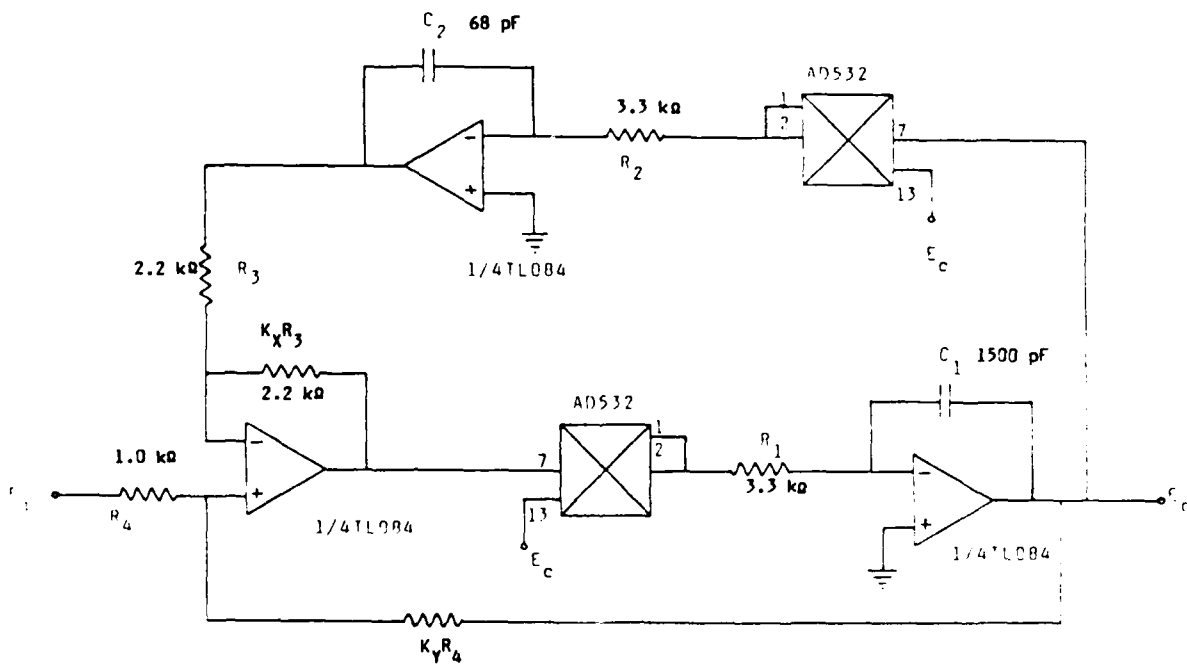
FIGURE 3 - Second-order tunable band-pass filter realized by two multipliers

Multipliers M_1 and M_2 are used to simultaneously vary the resistors R_1 and R_2 to obtain a linear variation of the resonant frequency as a function of the control voltage V_c and to maintain the Q factor constant. The Q factor and the gain are adjusted by the resistance $K_Y R_4$. Since the analog multipliers give an output normalized to 10 V, the relation between f_o and V_c is described by

$$f_o = \frac{1}{2\pi} \frac{V_c}{10} \left(\frac{K_X}{R_1 R_2 C_1 C_2}\right)^{\frac{1}{2}} \qquad [16]$$

The values of the components of the circuit of Fig. 2 allow the resonant frequency to be varied from 3 to 150 kHz as the control voltage V_c is adjusted to give 14 kHz/V. When this band-pass filter is built, we note that it breaks into free-running oscillations at high Q factors and high frequencies. Also, the measured values of the filter gain, quality factor and phase shift do not correspond to those calculated from these equations. These results can be explained if the nonidealities of the operational amplifiers and multipliers are taken into consideration. Real operational amplifiers normally have a gain and a phase-frequency response characterized by a single-pole model and the transfer function is

$$T(s) = \frac{A_o \omega_c}{s + \omega_c} \qquad [17]$$

The frequency response of real multipliers is given by

$$M(s) = \frac{E_c/10}{[1 + (s/\omega_m)]^2} \qquad [18]$$

For a typical low-cost operational amplifier as model TL074 from Texas Instruments, A_o is in the order of 100 dB and f_c is 10 Hz. For the AD532 multiplier from Analog Devices, f_m is in the order of 2.2 MHz.

The filter overall transfer function becomes more complicated if the functions $T(s)$, $M(s)$ and the output resistances of the two integrators, noted by r_o, are taken into account. Then, the transfer function can be written as

$$\frac{E_o(s)}{E_i(s)} = \frac{H_1 H_5}{1 - H_2 H_5 + H_3 H_5 H_6 + H_4} \qquad [19]$$

where $H_1 = T(s) \, K_Y / 1 + K_Y$,

$H_2 = T(s) \, M(s) / 1 + K_Y$,

$H_3 = T(s) \, K_X / 1 + K_X$,

$H_4 = T(s) / 1 + K_X$,

$H_5 = -T(s) \, M(s) \, (Z_1/r_o + Z_1)/(1 + T(s)) \, R_1/Z_1 + r_o)$, and

$H_6 = -T(s) \, M(s) \, (Z_2/r_o + Z_2)/(1+(1 + T(s)) \, R_2/Z_2 + r_o)$,

$r_o = 230 \; \Omega$ for the amplifiers TL084 from Texas Instruments,

$Z_1 = 1/s \; C_1$,

$Z_2 = 1/s \; C_2$.

The equality between eqs. 12 and 19 can be verified if we suppose that $T(s) = \infty$, $M(s) = 1$ and $r_o = 0$. In this case, the band-pass filter is composed of ideal components.

This transfer function, with the numerical value of the components specified in Fig. 3, is processed by a digital computer to calculate the factor Q and the filter gain. Curves 1 of Figs. 4 and 5 show that these factors increase as a function of the resonant frequency f_o. They remain relatively constant up to 10 kHz but, beyond this point, they increase rapidly and the filter becomes unstable before f_o attains 100 kHz. The circuit of Fig. 3 is then unable to cover the 5- to 140-kHz frequency band with a Q greater than 10.
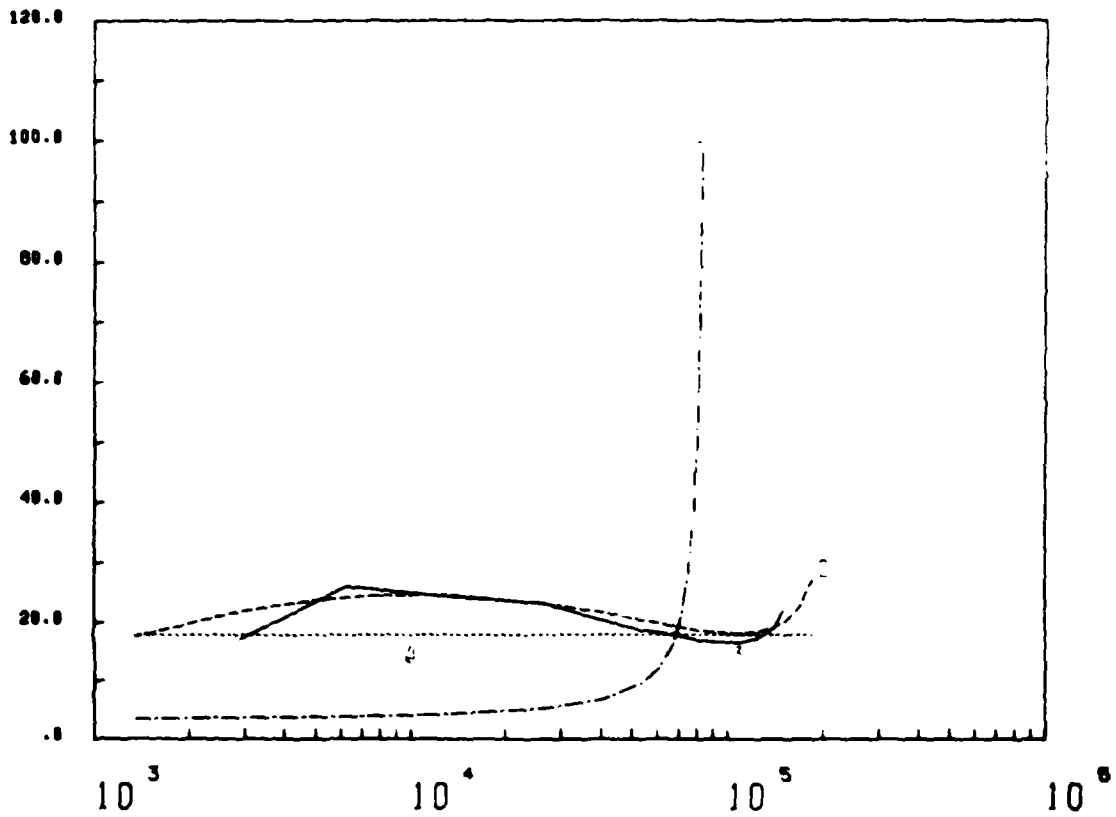
FIGURE 4 - Behavior of the quality factor of the band-pass filter as a
function of the resonant frequency f_o

Legend: —·—·—·—· 1 - transfer function computed without the third
                        multiplier
           — — — —   2 - transfer function computed with the third
                        multiplier
           ————————   3 - experimental measurements with the third
                        multiplier
           ········· 4 - ideal value
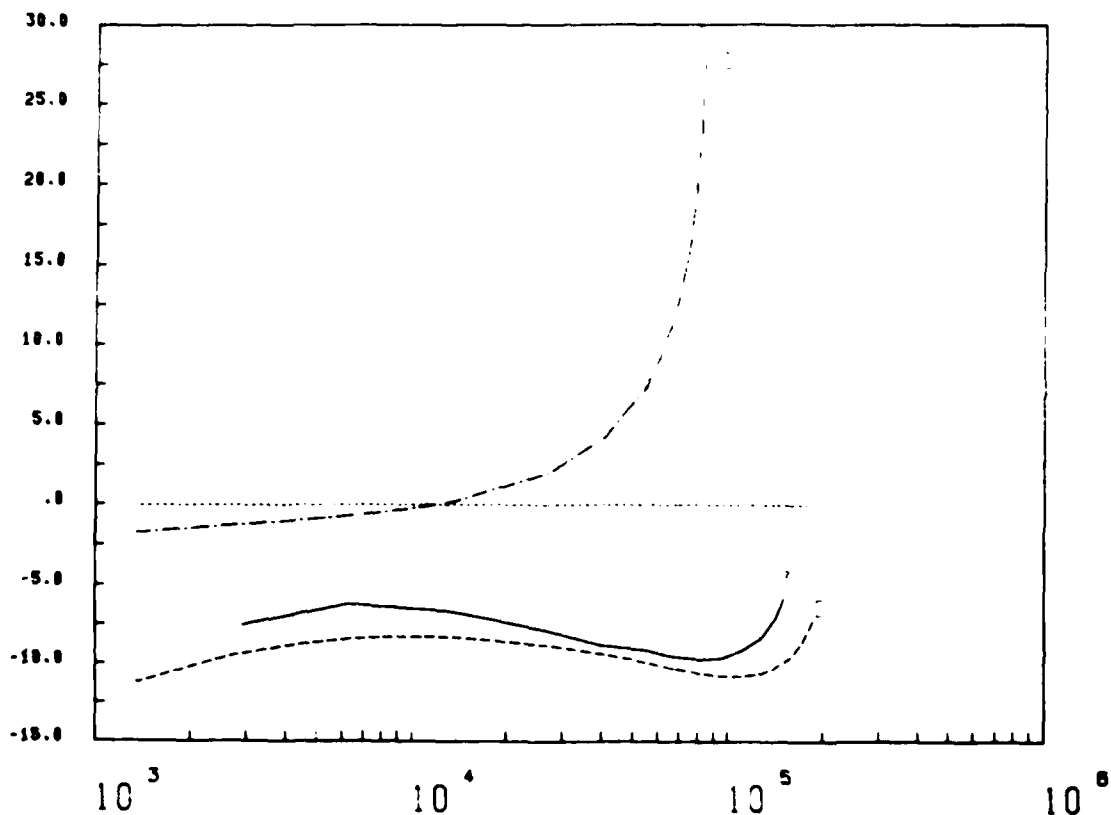
FIGURE 5 - Behavior of the gain of the filter as a function of the reso-
nant frequency

Legend: —•—•—•—• 1 - transfer function computed without the third
                          multiplier
           – – – – 2 - transfer function computed with the third
                          multiplier
           ———————— 3 - experimental measurements with the third
                          multiplier
           •••••••• 4 - ideal value
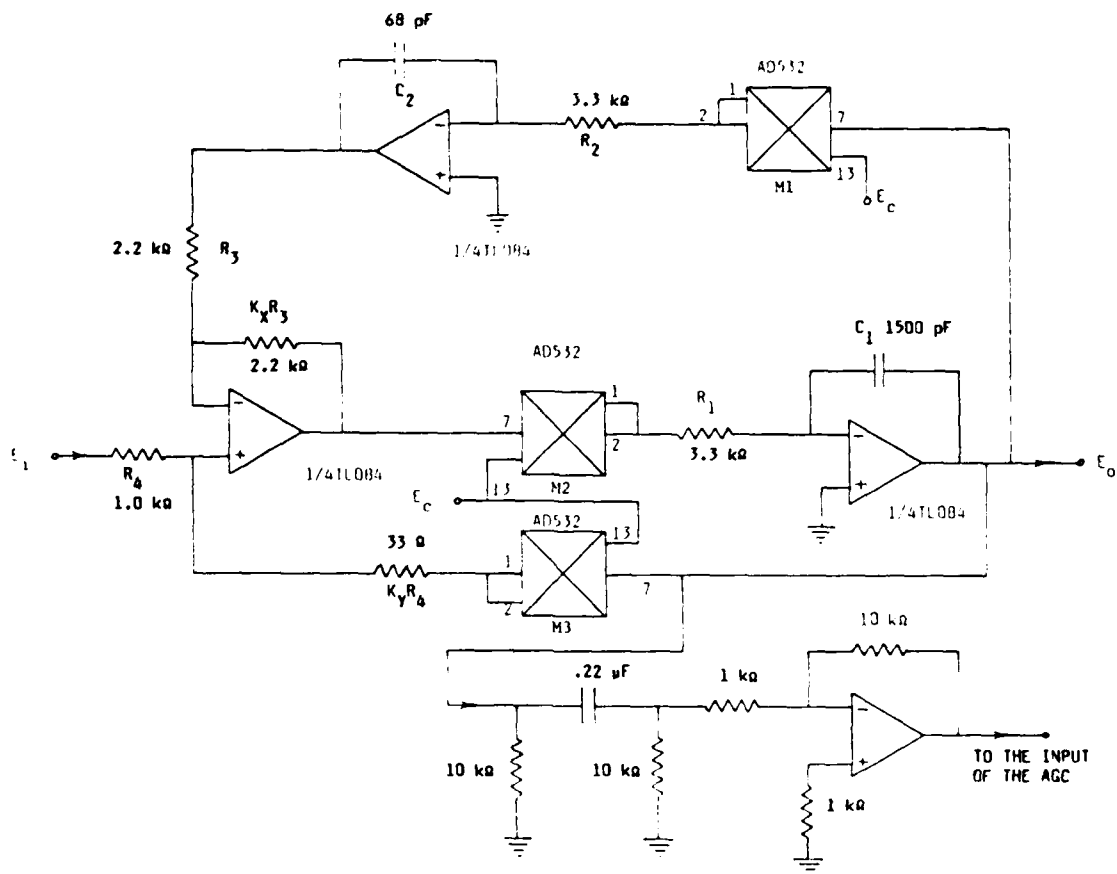
FIGURE 6 - Tunable band-pass filter whose resonant frequency is tuned by a control voltage and whose gain and quality factor are stabilized.

The increase of the quality factor and gain of the filter with f_o is a well-known phenomenon (Ref. 4) but not many solutions exist to maintain them constant (Refs. 5 and 6). Our solution (Fig. 6) is based on the assumption that the stabilization of the circuit can be obtained by decreasing the ratio K_Y as the tuning frequency is increased. This solution which modifies the circuit of Fig. 3 consists in adding a third multiplier to vary the factor K_Y with f_o. This multiplier is controlled by the voltage V_c that is used to change the resonant frequency of the filter.

An analysis of this circuit is realized by substituting in the transfer function of eq. 19 $H_2(s)$ by $M(s) H_2(s)$ to take into account this third multiplier. Curves 2 of Figs. 4 and 5 represent for this new transfer function the variation of the Q factor and gain as a function of the resonant frequency respectively. This analysis demonstrates that the circuit instability has been eliminated for high resonant frequencies and high Q's. It was determined experimentally that this filter can be continuously tuned from 3 to 150 kHz in maintaining the factor Q between 17 and 25 (Curve 3 of Fig. 4) and the gain between −6.2 and −9.8 dB (Curve 3 of Fig. 5). This represents the best performances that it is possible to obtain from this configuration. When the voltage V_c is small ($V_c < 0.25$ V), the ratio K_Y becomes too great, thus causing an instability which corresponds to a frequency smaller than 3 kHz. The analysis of the performances of this filter is completed by presenting in Fig. 7 the linearity of the control voltage V_c as a function of f_o that is obtained from the transfer function of eq. 19 (Curves 1 and 2) and by experimental measurements (Curve 3).

3.2 Tunable Band-Pass Filter with Operational Transconductance Amplifiers

The circuit illustrated in Fig. 8 shows an OTA used as a variable transfer function between the output E_o and the input E_1. If we let V_1 and V_2 be the positive and negative inputs of the amplifier, V_c the control voltage, V_{cc} the supply voltage and Z_R the load impedance, the output current I_o is controlled by the current I_c as related by the following equation

$$I_o = g_m I_c (V_1 - V_2) \qquad [20]$$

where $g_m I_c$ = transconductance value ($g_m \simeq 19.2$ V^{-1} for the OTA CA 3080 from RCA)

$$I_c = (V_c + V_{cc}) / R_c \qquad [21]$$
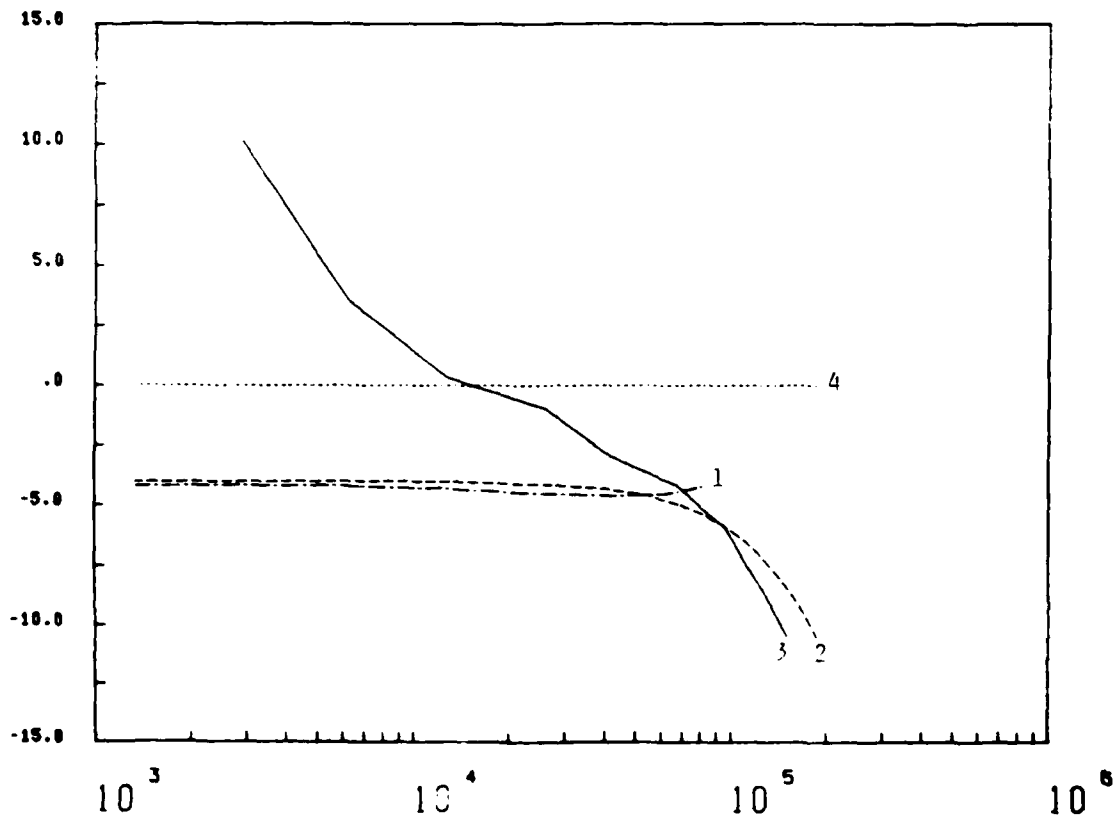
FIGURE 7 - Relative error of the control voltage as a function of the resonant frequency f_o

Legend: - - - - - 1 - transfer function computed without the third multiplier
- - - - 2 - transfer function computed with the third multiplier
———— 3 - experimental measurements with the third multiplier
.... 4 - ideal value
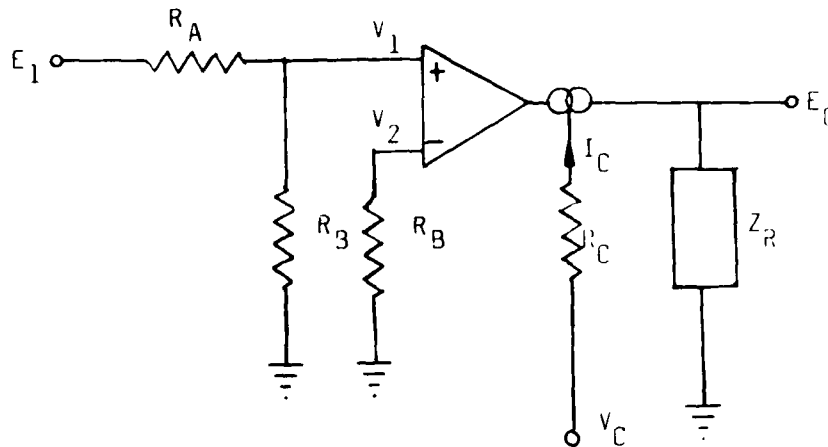
FIGURE 8 - Operational transconductance amplifier as a variable transfer
function

The transfer function between E_o and E_i is given by

$$\frac{E_o(s)}{E_i(s)} = g_m \cdot \frac{R_B}{R_A + R_B} \cdot \frac{(V_c + V_{cc})}{R_C} \cdot Z_R(s) \qquad [22]$$

For a linear operation, the values of R_A, R_B and R_C must be
determined in order to respect the following specifications: the maximum
values of the differential input voltage $(V_1 - V_2)_{max}$, the amplifier bias
current $(I_c)_{max}$ and the amplifier output current $(I_o)_{max}$. For the OTA
CA 3080, $(V_1 - V_2)_{max} \simeq 26$ mV, $(I_c)_{max} = (I_o)_{max} = 1$ mA.

As illustrated in Fig. 9, voltage-tunable active filters can be
produced by inserting two OTAs into the universal active filters. If
the outputs of OTAs are loaded by identical capacitors C_L, the voltage
transfer function between the band-pass output and the input is defined
as follows:

$$\frac{E_3(s)}{E_1(s)} = \frac{-(R_8/R_7)\,\omega_o\,s}{s^2 + (\omega_o\,R_8/R_5)\,s + \omega_o{}^2} \qquad [23]$$
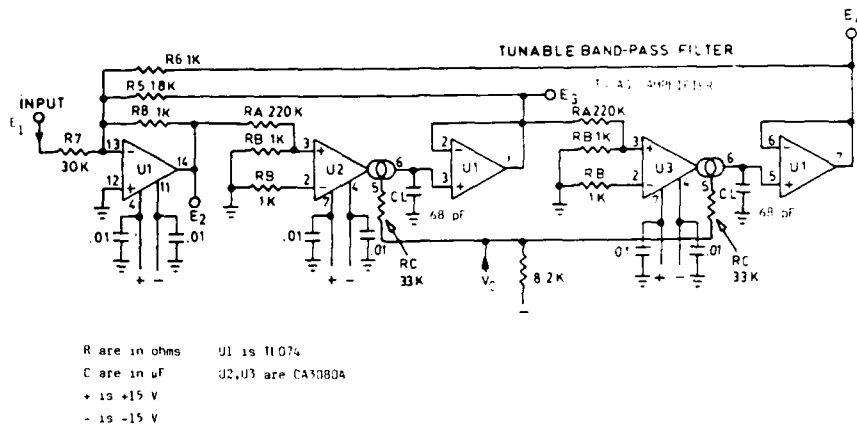
FIGURE 9 - Model of a second-order band-pass filter using operational
transconductance amplifiers

By comparing eqs. 12, 22 and 23, we find

$$\omega_o = \frac{g_m R_B (V_c + V_{cc})}{(R_A + R_B) R_c C_L} \qquad [24]$$

$$Q = R_5/R_8 \qquad [25]$$

$$K_F = R_5/R_7 \qquad [26]$$

The value of C_L is given by the maximum value of ω_o
corresponding to $(I_c)_{max}$. For the band-pass filter of Fig. 9, (E_1) max
= 6 V$_{peak}$, R_B = 1 kΩ, V_2 = 0 and $(f_o)_{max}$ = 200 kHz yield R_A = 230 kΩ and
C_L ≈ 68 pF.

The measured values of the quality factor Q and the gain of the
filter are plotted in Figs. 10 and 11 as functions of the resonant fre-
quency when the quality factor is set to 10, 15 and 18 respectively.
The expected value of the gain from eq. 25 is -6 dB. When the filter
operates with a Q smaller than 18, it does not require any compensation
to cover the 5- to 140-kHz frequency band. Under these conditions, the
quality factor and the gain of the filter can be maintain. quite con-

stant over this band. Finally Fig. 12, which is expressed as a per-
centage of the control voltage error between the expected and measured
values, shows that this error is limited to 5%.

However, the measured values of the gain filter and the quality
factor do not correspond exactly to those calculated from eqs. 24 and
25. The mismatch of these results can be explained by nonideal
operational amplifiers and OTAs. The OTA model in Fig. 13 takes into
account the input and output impedances noted by Z_i and Z_o and
assumes that the transconductance has a frequency response with a single
pole. Then, the transfer function of the OTA becomes

$$T_1(s) = \frac{E_o(s)}{E_i(s)} = g_m(s) \cdot \frac{Z_o Z_L R_B Z_i (V_c + V_{cc})}{(Z_o + Z_L)(R_B^2 + Z_i(R_A + R_B) + 2R_A R_B)R_c} \qquad [27]$$

where

$$g_m(s) = \frac{g_m \, \omega_{OTA}}{s + \omega_{OTA}} \qquad [28]$$

$$Z_L = \frac{1}{C_L s}$$

If the T(s) functions for operational amplifiers and $T_1(s)$ ones
for OTAs are considered in the filter of Fig. 9, the overall transfer
function between the band-pass output and input can be written as

$$\frac{E_3(s)}{E_1(s)} = \frac{H_A(s) \, T_2(s)}{1 - T_2(s) H_B(s) - T_2^2(s) H_C(s)} \qquad [29]$$

where

$$H_A(s) = \frac{-R_8/R_7}{1 + (R_8 + R_7)/R_7 T(s)}, \qquad T_2(s) = \frac{T_1(s) \, T(s)}{1 + T(s)},$$

$$H_B(s) = \frac{-R_8/R_5}{1 + (R_8 + R_5)/R_5 T(s)}, \qquad H_C(s) = \frac{-R_8/R_6}{1 + (R_8 + R_6)/R_6 T(s)}.$$
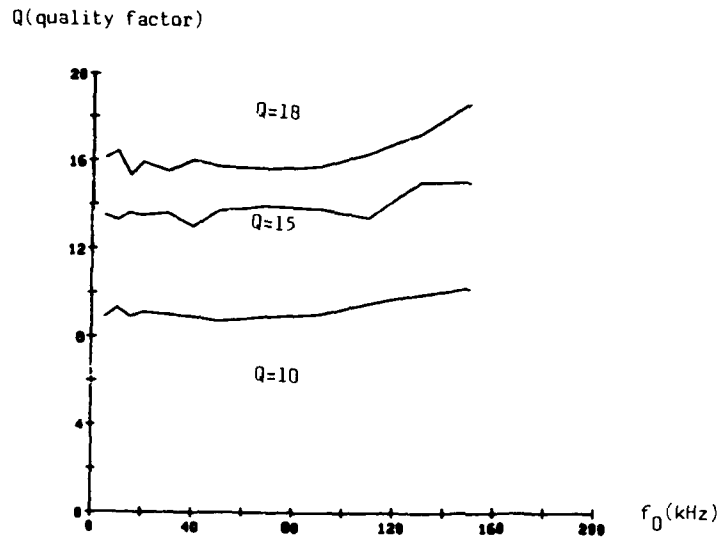
Q(quality factor)

FIGURE 10 - Behavior of the quality factor of the band-pass filter built with OTAs as a function of the resonant frequency for various values of Q

GAIN(dB)
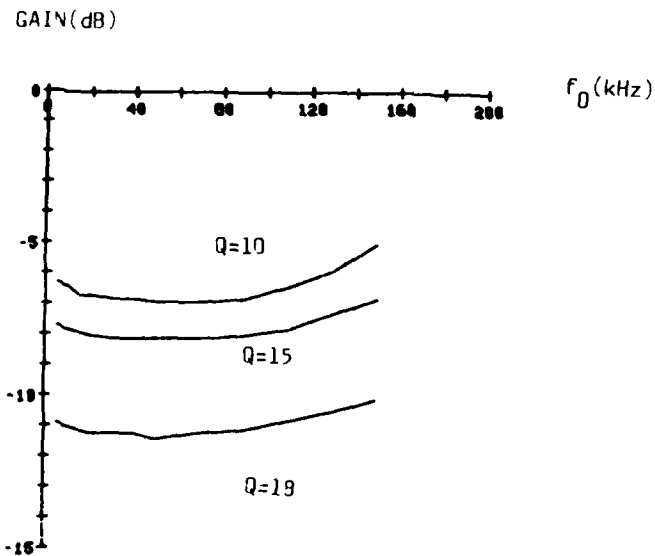
FIGURE 11 - Behavior of the gain of the filter built with OTAs as a function of the resonant frequency when the factor of quality is set to 10, 15 and 18.

Control voltage error (in %)
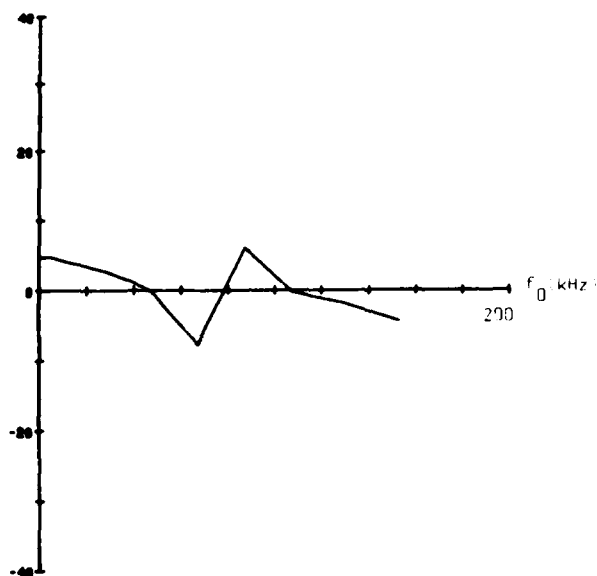
FIGURE 12 - Relative error of the resonant frequency control voltage of the band-pass filter built with OTAs as a function of the resonant frequency

$I_0 = \epsilon g_m(s) I_c$

E_i

R_A

ϵ Z_{in}

R_B

R_B

I_0

$I_c = \dfrac{V_c + V_{cc}}{R_c}$

Z_0 Z_L

$T(s)$

E_0
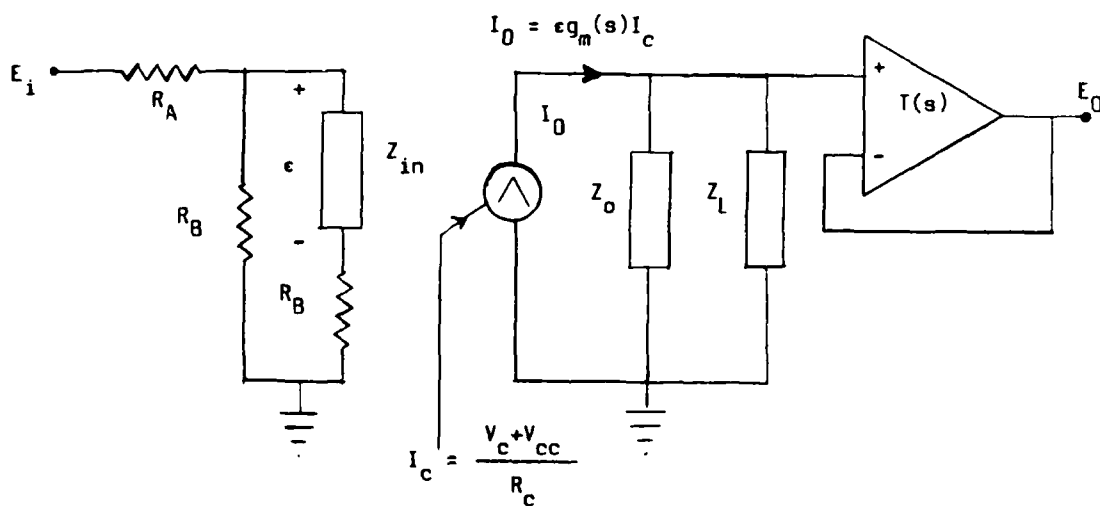
FIGURE 13 - Model of a nonideal operational transconductance amplifier

To maintain the gain and the quality factor more constant when varying the resonant frequency, the filter can be easily compensated by replacing the capacitor C_L at the output of the two integrators by a network that produces a phase advance. This network can be a serial combination of a resistor R_L with the condenser C_L whose transfer function is

$$Z_L(s) = (R_L \; C_L \; s + 1)/C_L s$$

3.3 Automatic Gain Control Amplifier

The AGC amplifier adjusts the output of the band-pass filter to a reference level compatible with the driving signal of the F/V converter. This amplifier, which is illustrated in Fig. 9, maintains its output at a fixed amplitude by controlling the gain of an OTA. The output of the OTA is full-wave rectified and filtered by a circuit characterized by a fast-charge and a slow-discharge behavior. Then, the signal is compared to a reference voltage to produce an error voltage which, after being low-pass filtered, adjusts the gain of the OTA.

An ideal OTA gives an output varying as a function of the control voltage E_c and its input voltage V_1. In the schematic of Fig. 14, its transfer function is

$$V_o(s) = K \; (E_c(s) + V_A) \; V_1(s) \qquad [30]$$

where $\quad K = \dfrac{g_m \; R_9 R_{11} (R_{12} + R_{13})}{(R_9 + R_{10}) R_{12} R_{21}}$

$g_m \approx 19.2 \; V^{-1}$ for the amplifier CA 3080 from RCA,

$V_A = V_{cc} - V_Z$,

V_{cc} = the supply voltage (15 V),

V_Z = the reverse breakdown voltage of the Zener diode D_6 (≈ 5.1 V for the diode 1N751A).

FAST AUTOMATIC GAIN CONTROL AMPLIFIER (FAGC)
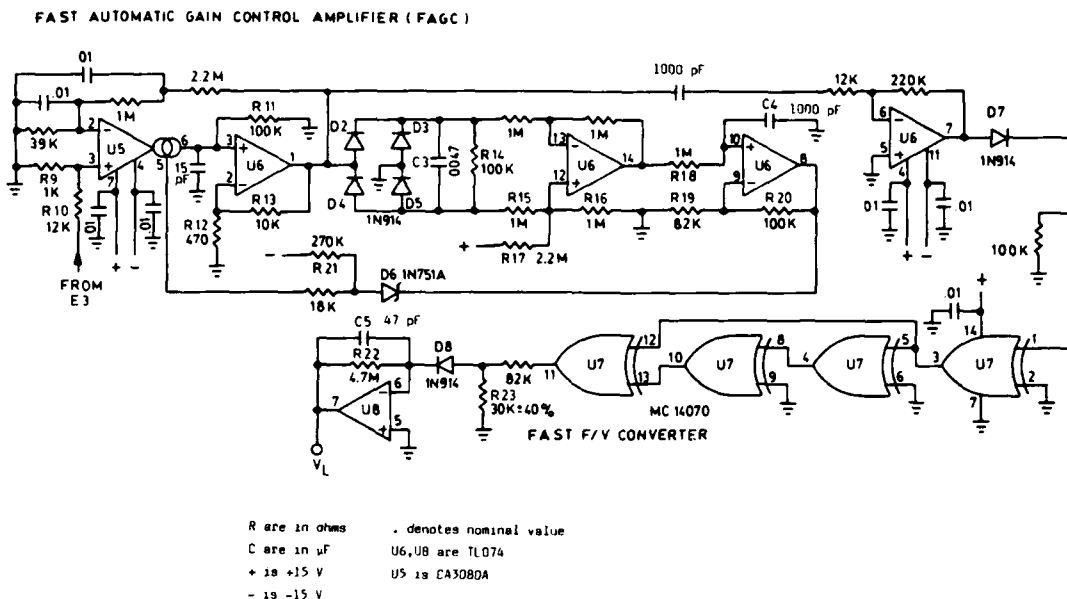
FIGURE 14 - Automatic gain control amplifier and frequency-to-voltage
converter

The voltage bias, that is created by the Zener diode D_6, allows
the control current I_c of the OTA to be varied from 0 to $(I_c)_{max}$
(≈1 mA). Consequently, this bias increases the dynamic range of the AGC
amplifier.

The control voltage E_c is defined as a function of the refer-
ence amplitude V_R, the peak voltage of the input signal V_{1p} and the time
constants of the two filters of the control loop.

$$(E_c(s) + V_A) = \frac{K_y V_R / \tau_2 \; s + 1}{1 + K_y K \; V_{1p}/(\tau_1 \; s + 1) \; (\tau_2 \; s + 1)} \qquad [31]$$

where $K_y = (R_{19} + R_{20})/R_{19}$

$$V_R = V_{cc} \frac{R_{15}}{2R_{17} + R_{15}}$$

$$\tau_1 = R_{14}C_3$$

$$\tau_2 = R_{18}C_4$$

Then, the gain of the AGC amplifier is found by combining eqs. 30 and 31:

$$\frac{V_0(s)}{V_1(s)} = \frac{K\,K_y V_R/(\tau_2 s + 1)}{1 + K\,K_y V_{1p}/(\tau_1 s + 1)(\tau_2 s + 1)} \qquad [32]$$

The amplitude dynamic range (R) of the AGC amplifier is derived from eq. 30 and its value is given by the relation

$$R_{dB} = 20\ \log\ K\big[\Delta(E_c + V_A)\big] \qquad [33]$$

where $\quad V_Z - V_{cc} < E_c < V_R$.

Then,

$$R_{dB} = 20\ \log\ \big[K(V_R + V_{cc} - V_Z)\big] \qquad [34]$$

The time constant T_{AGC} of the AGC amplifier is defined as the time required by the output amplitude (or by the control voltage E_c) to complete 63.2% of its total rise (or decay) when the input is forced by a step in amplitude. It is derived from eq. 32 and its value is

$$\tau_{AGC} = -\tau_2\ \ell n\Big[\frac{e^{-1}(\tau_2 - \tau_1)}{\tau_2 - \tau_1 e^{-\tau_2/\tau_1}}\Big] \qquad [35]$$

where $\quad \tau_2 > \tau_1$.

The output waveform, after being processed by a low-pass filter, feeds back the negative input of the OTA. This configuration attenuates the DC voltage and low-frequency fluctuations that accompany the output.

3.4 Frequency-to-Voltage Converter and Voltage Adaptor

The output of the AGC amplifier is adjusted to present a saturated waveform to the input of the F/V converter. The gain of this amplifier must be set at V_{cc}/V_R. Then, the converter transforms this signal into a train of short-duration pulses by using exclusive OR (EXOR) gates and delay operation (see Fig. 14). Since pulses are generated on the rising and falling edges of the input waveform, the repetition rate of pulses is twice greater than the frequency of the input signal. Pulses are averaged through a low-pass filter (of time constant τ_1) yielding the output voltage V_L. It is so adjusted to give 0.0714 V/kHz.

The transfer function between the F/V output and its input frequency is given by

$$\frac{V_L}{\omega_j} = \frac{K_2}{\tau_3 s + 1} \qquad [36]$$

where $\tau_3 = R_{22}C_5$.

An operational amplifier low-pass filters the F/V output and adapts it to the voltage V_c that controls the resonant frequency of the band-pass filter (Fig. 15). The transfer function of this adaptor is related as

$$V_c(s) = \frac{K_3 V_L(s)}{\tau_4 s + 1} + K_4 \qquad [37]$$

where $\tau_4 = C_6 R_{24}$.
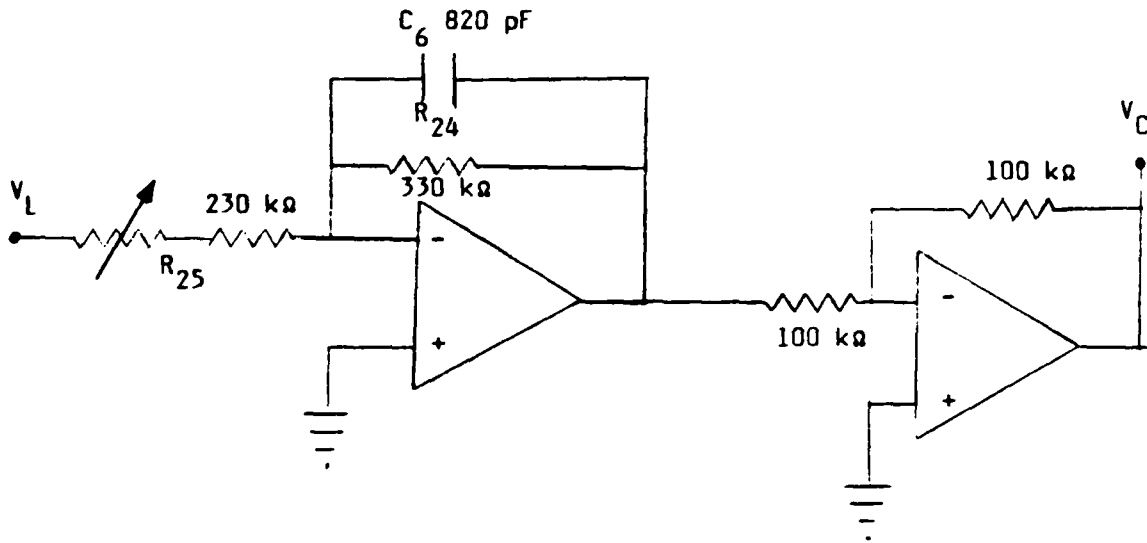
a) for band-pass filter built with multipliers
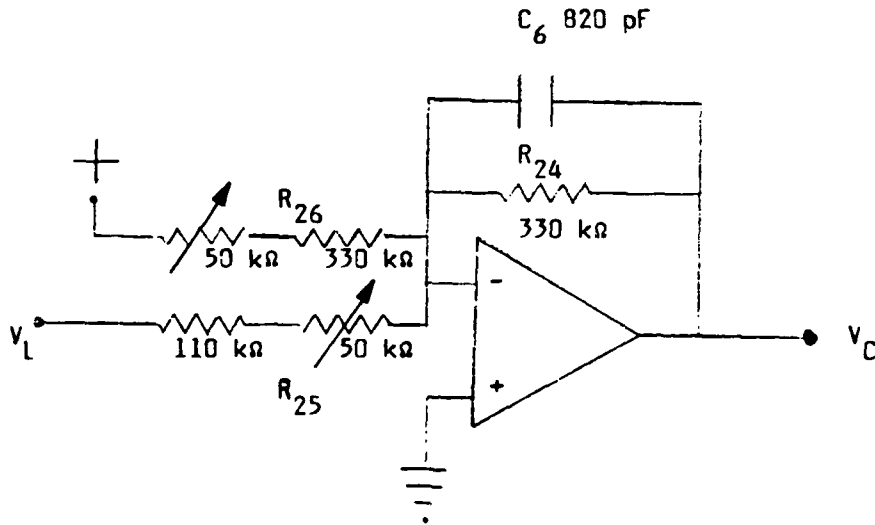
b) for band-pass filter built with operational transcon-
ductance amplifiers

FIGURE 15 - Voltage adaptor to match the output of the F/V converter to
that of the control voltage of the band-pass filter

The transfer function between the input frequency ω_j of the F/V converter and the control voltage V_c is obtained by combining eqs. 36 and 37. This yields

$$V_c(s) = \frac{K_2 K_3 \omega_j(s)}{(\tau_3 s + 1)(\tau_4 s + 1)} + K_4 \qquad [38]$$

If the band-pass filter with multipliers is used, eq. 16 proves that $K_4 = 0$ and K_3 must be adjusted to give $10/\sqrt{K_X/R_1 R_2 C_1 C_2}$.

For the band-pass filter built with OTAs, eq. 24 highlights that the parameters K_3 and K_4 must be set to $(R_A + R_B) R_C C_L/g_m R_B$ and to $-V_{cc}$ respectively. Variable resistances R_{23}, R_{25} and R_{26} allow the setting of parameters K_2, K_3 and K_4.

The time constant of the frequency-tracking loop (τ_L) is then derived from eq. 25. The value of τ_L is:

$$\tau_L = -\tau_4 \ln \left[\frac{e^{-1}(\tau_4 - \tau_3)}{\tau_4 - \tau_3 e^{-\tau_4/\tau_3}} \right] \qquad [39]$$

where $\tau_4 > \tau_3$.

The derivation of pulses within the F/V converter is determined by the propagation delay time t_{pHL} (or t_{pLH}) which is the time between the specified reference points, normally 50% of the points on the input and output voltage waveforms, with the output changing from the defined low level to the defined high level (or the defined high level to the defined low level).

The F/V output V_L is determined by the duration of pulses. Since this duration is proportional to t_{pHL} (or t_{pLH}), eq. 36 can be rewritten as

$$V_L(s) = \frac{(4K_5 V_{cc} t_{pHL}) \omega_j}{\tau_3 s + 1} \qquad [40]$$

where $4 V_{cc} \tau_{pHL} \omega_j$ is proportional to the average of pulses and K_5 is the gain that is adjusted to give 0.0714 V/kHz. We assume that $t_{pHL} = t_{pLH}$. From the curves of Ref. 7, we deduce that the delay time of gates MC14070 can be approximated by the linear relation

$$t_{pHL} = 15 + \frac{1}{18} (T + 60) \text{ ns} \qquad [41]$$

where t_{pHL} is specified in nanoseconds and T in degrees Celsius.

Then eqs. 40 and 41 show that the F/V output can vary as a function of temperature. For example, if the F/V output is initially adjusted to 20°C, it will change at a rate of approximately 0.30%/°C because of the change in pulse width.

The F/V converter transforms the output of the AGC amplifier in a train of short-duration pulses. These pulses are filtered by an RC circuit characterized by fast-charge and slow-discharge behaviors. Ripple voltage ri(t) can be observed at the output of the F/V converter and it has been lowered by using a pulse-rate doubler (maintaining a ratio of two between the repetition rate of pulses and the input frequency). The ripple voltage is a function of the time constant of the F/V converter and is expressed as

$$ri(t) = v_L(t) (1 - e^{-t/2\tau_3}) \qquad [42]$$

where $0 < t < 1/f_j$.

We assume in eq. 42 that the duration of pulses is negligible compared to the period of the input frequency f_j. The peak-to-peak value of the ripple voltage is given by

$$ri_{pp} = v_L(t) \ (1-e^{-1/2 \ f_j \tau_3}) \qquad [43]$$

We note from eq. 42 that the ratio $ri(t)/v_L(t)$ increases as the input frequency decreases. In maintaining the term $1/2 \ f_j \tau_3$ smaller than two, the value $ri(t)$ is quite constant for the entire bandwidth.

4.0 DESIGN EXAMPLE AND ITS PERFORMANCE

The tracking filter of Fig. 16 operates with the best specifications that can be obtained from such a configuration. The quality factor of the band-pass filter built with the OTAs is set to about 15 and the time constants of the AGC amplifier and the F/V converter are set to 1 ms and 500 µs respectively. The specifications of the tracking filter are presented in Table I.

The tracking filter was subjected to several laboratory tests to determine its dynamic range, its frequency agility and its immunity to noise and interference signals. As shown in Table II, it has been necessary to identify two maximum excitations for the tracking filter, one required to lock the processor and another to maintain lock. These voltages have been measured at several frequencies within the bandwidth of the processor.

In the laboratory, the frequency agility was measured by feeding the output of a programmable signal generator through the tracking filter. As shown in Fig. 17, the processor reacts correctly to enormous sinusoidal swings in frequency, namely 15-140, 60-120 and 10-40 kHz. Various ratios $\Delta f/f_c$ are used and the shape of the curves of Fig. 2 are verified experimentally. The frequency of the sweep from 15 to 140
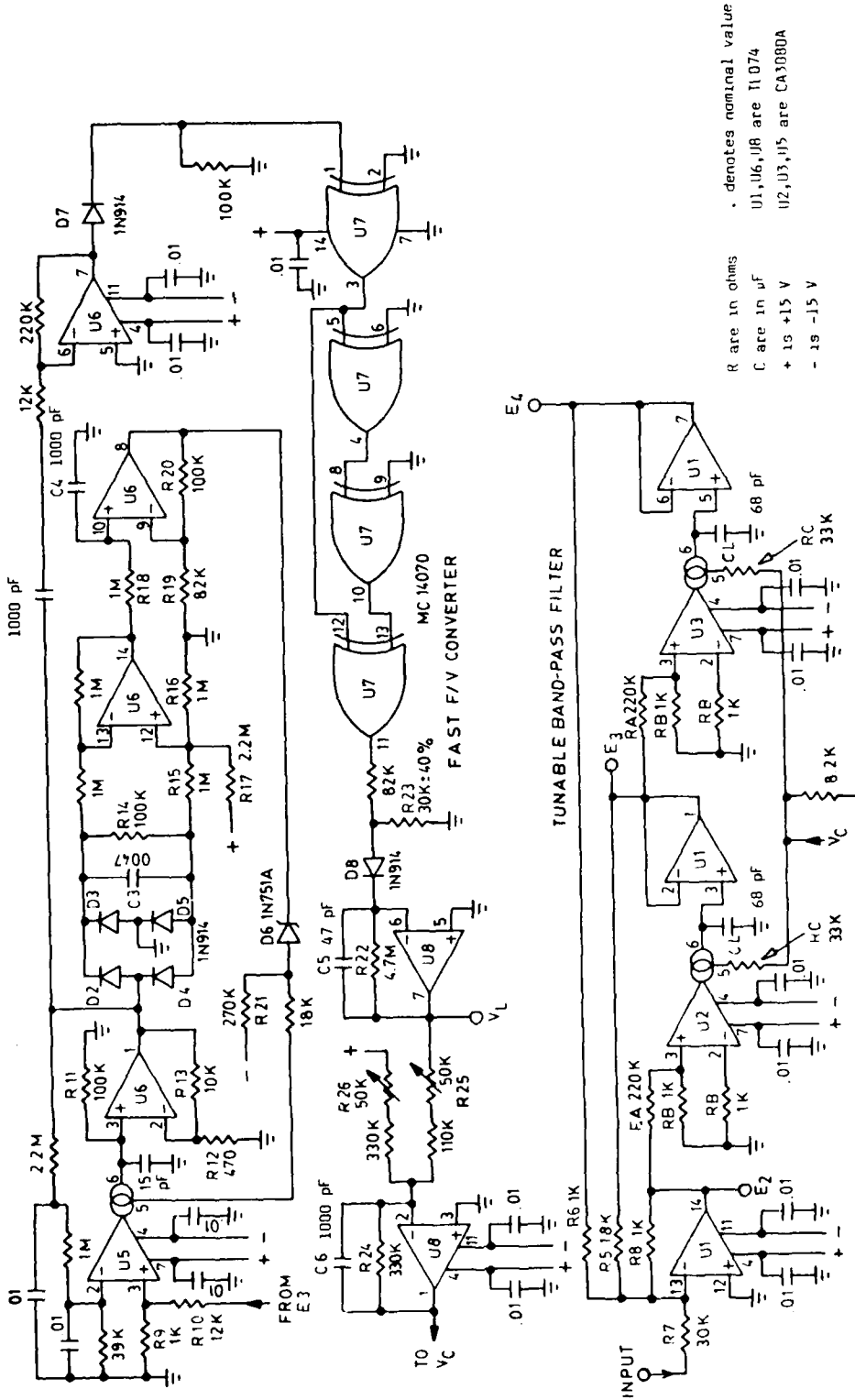
FIGURE 16 – Frequency-tracking filter whose band-pass filter is built with operational transconductance amplifiers.

TABLE I

Specifications of the frequency-tracking filter and its components

FREQUENCY-TRACKING FILTER	
Voltage supplies	±15 V, 2 W
Frequency range	4–140 kHz
Maximum input voltage	10 V r.m.s.
Minimum input voltage	(see Table II)
TUNABLE BAND-PASS FILTER	
Frequency range	4–150 kHz
Dynamic range	(see Table II)
Maximum input voltage	30 V peak-to-peak
Quality factor Q	16 to 21
Gain	−4.9 to 2.7 dB
AUTOMATIC GAIN CONTROL AMPLIFIER	
Frequency range	5–200 kHz
Dynamic range	55 dB
Time constant	1 ms
FREQUENCY-TO-VOLTAGE CONVERTER	
Dynamic range	2–195 kHz
Ripple on averaged output	150 mV (peak)
Time response to a frequency step	500 μs
Minimum input voltage	3 V peak-to-peak

TABLE II

Minimum amplitudes required for lock-on and maintenance of
lock of the band-pass filter as a function of frequency

Frequency	Minimum voltage (peak-to-peak)	
	for lock-on	for maintenance of lock
(kHz)	(V)	(V)
5	1.6	0.2
10	1.0	0.1
15	0.36	0.11
20	0.22	0.1
25	0.12	0.1
40	0.11	0.085
50	0.1	0.075
70	0.1	0.09
80	0.15	0.1
90	0.36	0.16
110	0.5	0.32
130	0.34	0.25
140	0.56	0.16

(a)
15-140 kHz

(b)
60-120 kHz

(c)
10-40 kHz

5 ms/div

5 ms/div

20 ms/div

5 ms/div

1 ms/div

5 ms/div

2 ms/div

0.5 ms/div

2 ms/div
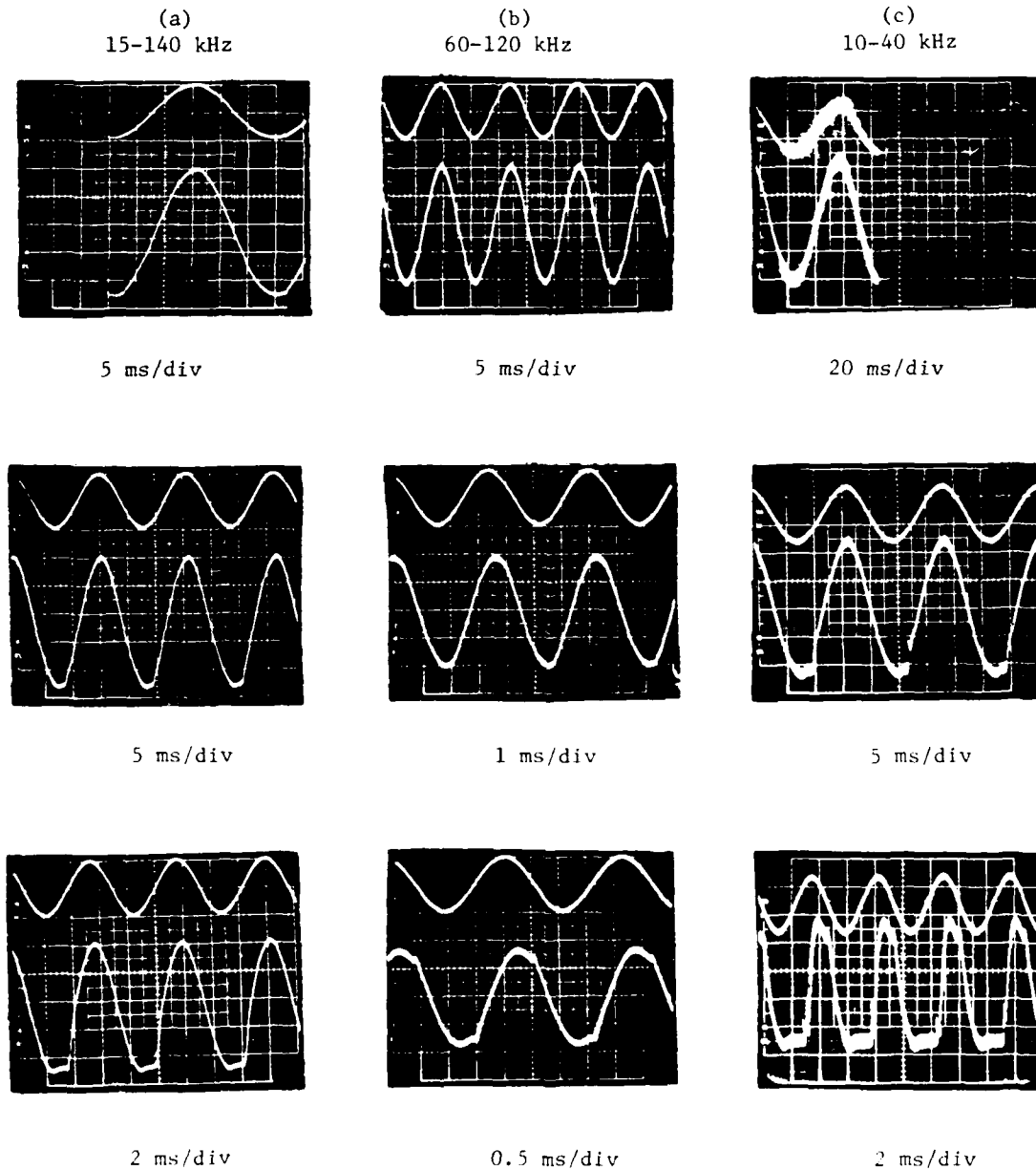
FIGURE 17 - Results of the agility tests to which the tracking filter was
subjected. At (a), a sinusoidal frequency sweep from 15 to
140 kHz is applied at 35, 60 and 150 Hz respectively; at (b),
a sinusoidal frequency sweep from 60 to 120 kHz is applied at
75, 275 and 450 Hz; at (c) a sinusoidal frequency sweep from
10 to 40 kHz is applied at 16, 55 and 200 Hz. In each case,
the upper trace represents the modulation of the frequency
generator while the lower trace is the actual voltage at the
output of the F/V converter.

kHz and from 10 to 140 kHz was limited by the dynamic amplitude range of the AGC amplifier. In the other case, the frequency of the sweep was limited by the time constant of the amplifier. When the limit in the frequency of the sweep is attained, the output waveform is slightly delayed and distorted.

The immunity of the processor to noise and interference signals has also been measured in the laboratory. In a first test, the processor has been initially locked on to a signal and the level of white noise was increased until loss of lock. Repeated at several frequencies, this test revealed that the processor remains locked as long as the signal-to-noise ratio remains above -14 dB.

In a second test, its resistance to interference signals was measured in the following manner. The processor was first locked on to a signal of strength S_1 at frequency f_1, then another signal of strength S_2 at frequency f_2 was added to the input while increasing S_2 until loss of lock on the first signal occurred. This test was repeated for several frequencies f_1 and f_2 as follows :

f_1(kHz)	f_2(kHz)	S_1/S_2(dB)
90	30	-24
60	30	-20
30	90	-20
60	90	-18

The situation where f_1 and f_2 vary with time was simulated by locking the filter onto S_1 at f_1 and letting f_2 grow coincidently with f_1 and pass this frequency. The filter has always remained locked on S_1 when the ratio S_1/S_2 remained above 4 dB.

5.0 APPLICATION OF THE TRACKING FILTER TO A DOPPLER SIGNAL PROCESSOR

To demonstrate the capability of the filter to track the frequency of a signal in presence of interference, let us inject into this filter the Doppler signal from magnetic tape recordings of telemetry data. These signals were obtained from instrumented RIM-7E5 missile firings.

The RIM-7E5 missile guides itself towards the target by using radar as the signal source for semiactive homing. Since there is no transmitter in the missile, its guidance depends on the RF energy radiated by an illuminator and on the reflection of that energy by the target. The illuminator signal, used as reference, and the reflected signal are received by the rear and front antennas respectively and are processed in the missile to derive directional, range and velocity information. This information is contained in the video Doppler signal, a low-frequency one (5-140 kHz), whose frequency is proportional to the missile target closing velocity. This signal is difficult to track since it contains in addition to the target return, clutter, jet engine modulation (JEM) and receiver noise.

During flight, the frequency content of the Doppler signal varies continuously. During boost, the Doppler frequency of the target increases because of missile acceleration while it slowly decreases during the glide phase because of missile deceleration. At intercept, there is a rapid change in the frequency content of the target return due to the geometry of the intercept. This transient is called the Doppler roll-off and its duration is proportional to the rate of change of the line of sight to the target during intercept (ratio of missile-target closing velocity to miss distance).

Figures 18 to 20 show the spectral content of various Doppler signals that have been derived from a real-time spectrum analyzer. The

reaction of the tracking filter to these Doppler signals is given by recording the output of the F/V converter as a function of time. A common signal allows synchronizing both displays.

Consider Fig. 18; the Doppler signal is characterized by a long roll-off (72 ms from 0.9 f_{do} to 0.5 f_{do}) where f_{do} is the preintercept target Doppler frequency and the 0.5 f_{do} corresponds to the time of closest approach. Examination of the data reveals that the tracking filter follows the target Doppler frequency during the intercept phase in eliminating interference such as JEM and clutter. Figure 19 has been obtained under the stimulus of a Doppler signal characterized by a very short roll-off which results from a miss distance of 0.3 m. For this case, the output of the F/V converter demonstrates that the tracking filter is fast enough to follow the target return. Finally, Fig. 20 presents much more difficult conditions where the target return is mixed with very strong returns from JEM and clutter. It is shown that the tracking filter reacts correctly in extracting the target return from this complex Doppler signal.

50 kHz —

Output of the F/V converter

0 kHz —

100 ms

50 kHz —

Frequency content of the Doppler signal
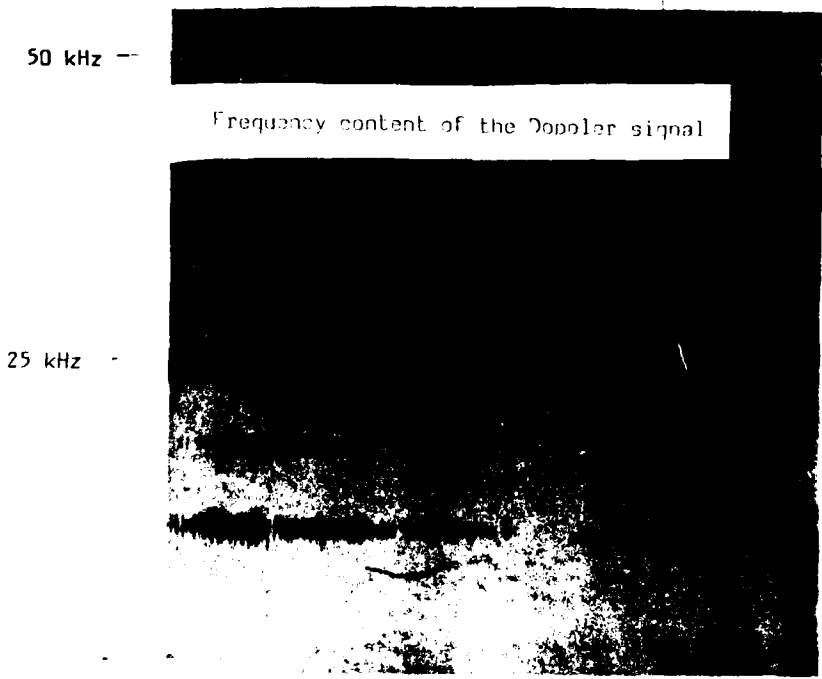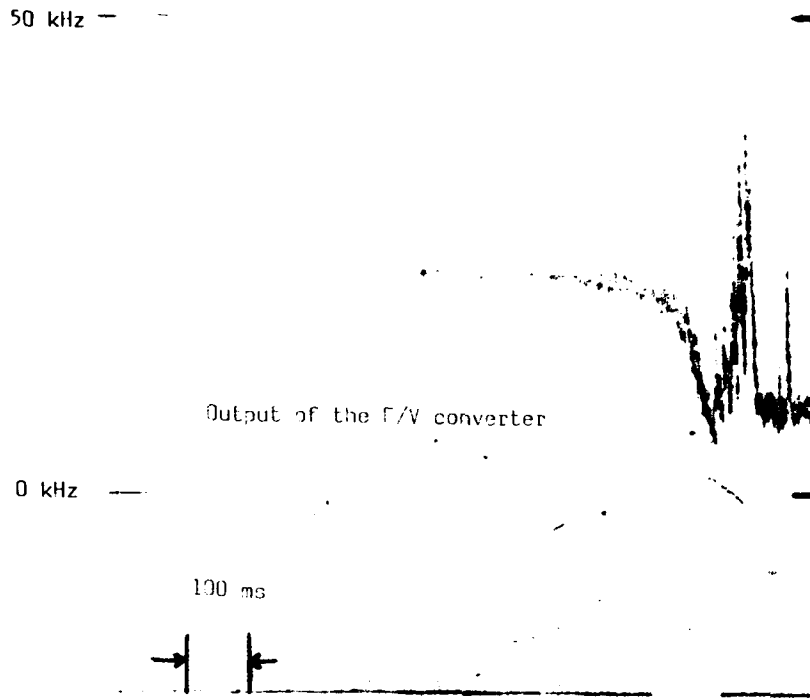
25 kHz —

FIGURE 18 - Response of the frequency-tracking filter to a Doppler signal
characterized by a long roll-off

50 kHz — —

Output of the F/V converter

0 kHz — —

10 ms

50 kHz —

Frequency content of the Doppler signal

25 kHz —
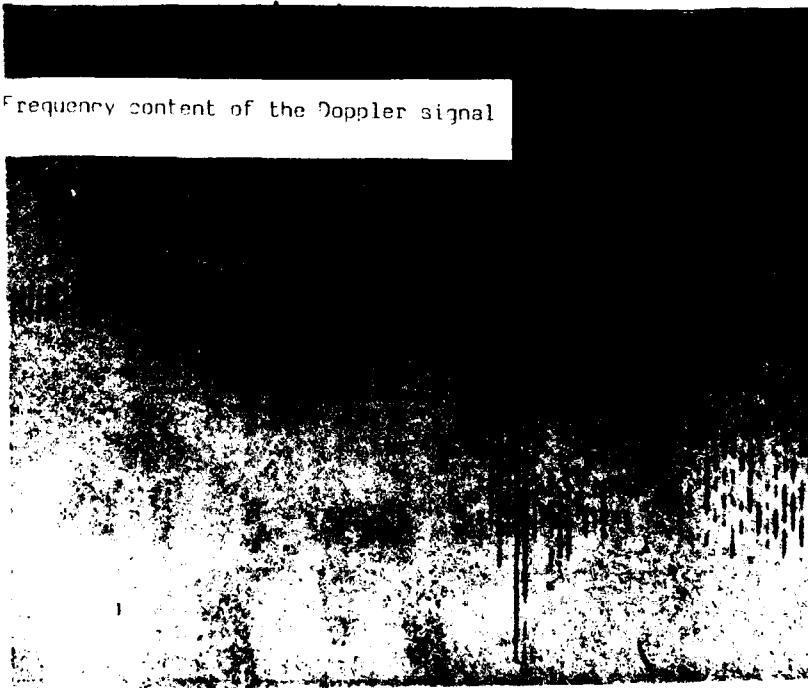
FIGURE 19 - Response of the frequency-tracking filter to a Doppler signal
characterized by a short roll-off

50 kHz——

Output of the F/V converter

0 kHz ——

10 ms

50 kHz -

25 kHz -

Frequency content of the Doppler signal
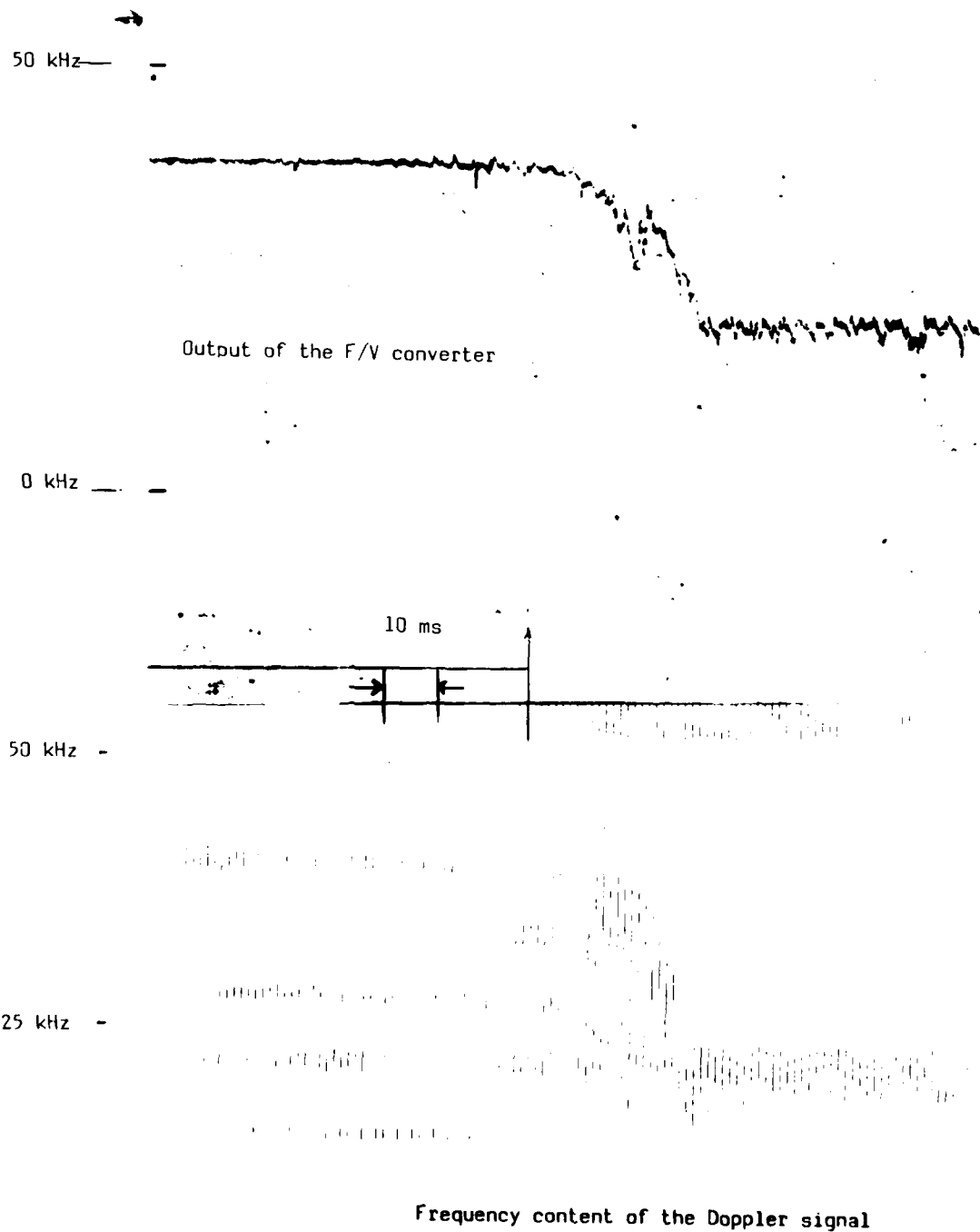
FIGURE 20 - Response of the frequency-tracking filter to a Doppler signal
characterized by strong interference

6.0 CONCLUSION

The feasibility of frequency-tracking filters operating in the 5- to 140-kHz frequency range was demonstrated. System analysis provides insight into the parameters that essentially determine the performance of the filter. Each component of the proposed frequency-tracking filter has been fully described and analyzed. The band-pass filter has been designed to exhibit a constant quality factor and a constant resonant-frequency gain. The AGC amplifier and the F/V converter have been built to perform fast time responses.

Experimental results were derived from a tracking filter operating with a quality factor of 15 and with a time constant of the AGC amplifier and F/V converter set at 1 ms and 500 µs respectively. The immunity of the system to white noise is established at -14 dB. It was determined that, if the filter is initially locked on to a signal at 90 kHz, it can reject an interference located at 30 kHz provided that the signal-to-interference ratio (S_1/S_2) is greater than -24 dB. In addition, the tracking filter can reject an interference located between the starting and final points of a frequency sweep if the amplitude ratio S_1/S_2 is greater than 4 dB. Otherwise, it is possible that the filter remains locked on to the interference at the crossing time. The test of frequency agility demonstrates that the filter can track a signal whose frequency is varied from 60 to 120 kHz at a rate of 200 Hz.

Such a tracking filter is used to process a Doppler signal whose frequency content is composed of the target return and strong interference such as jet engine modulation and sea clutter. At intercept, the Doppler frequency shifts to about one half of the preintercept frequency. It is shown that the filter is sufficiently immune to noise and interference and is frequency-agile enough to track the Doppler frequency of the target return before and during the intercept phase of a semiactive guided missile.

7.0 REFERENCES

1. Lindquist, C.S. and Gocal, G., "A Simple Tracking Filter", Conf. Record of the Twelfth Asilomar Conf. on Circuits, Systems and Computers, pp. 24-28, 1978.

2. Sedra, A.S. and Sparkes, R.G., "A Tracking Biquad Active Filter", Proc. of the 1974 IEEE International Symposium on Circuits and Systems, New York, pp. 585-589, 1974.

3. Wong, Y.J. and Ott, N.F., "Functions Circuits, Design and Applications", Burr-Brown Research Corporation, McGraw-Hill Book Company, New York, pp. 222-226, 1976.

4. Thomas, L.C., "The Biquad: Part 1, Some Practical Design Considerations", IEEE Trans. Circuit Theory, Vol. CT-18, No. 3, pp. 350-377, May 1971.

5. Hurtin, G., "Voltage Tunable Multipole Band-Pass Active Filters", Proceedings of the 1974 IEEE International Symposium on Circuits and Systems, New York, pp. 569-572, April 1974.

6. Shaumgan, R., "Low-Sensitivity High-Frequency Tunable Active Filter Without External Capacitors", IEEE Trans. Circuits and Systems (USA), Vol. CAS-22, No. 1, pp. 39-44, January 1975.

7. "CMOS Data Book", Fairchild Camera and Instrument Corporation, Mountain Viero, California, 1977.

DREV R-4347/85 (UNCLASSIFIED)

Research and Development Branch, DND, Canada.
DREV, P.O. Box 8800, Courcelette, Que. GOA 1R0

"An Active Tracking Band-Pass Filter" by A. Morin and P. Labbé

A frequency-agile tracking filter, which operates over a wide frequency range with a high immunity to noise and interference, has been designed. It consists of a second-order band-pass filter which is continuously tunable over the 5- to 140-kHz band. The resonant frequency of the filter is adjusted by means of a feedback loop to the frequency component of greatest amplitude in the input signal. The loop includes a fast AGC amplifier, a fast frequency-to-voltage converter and a low-pass filter. The components of the tracking filter are described and analyzed. Analysis of the tracking filter, as regards its immunity to noise and interference, its frequency agility and the stability of its control loop, is also presented to optimize system parameters. Finally, the performance of the processor is shown by experimental measurements.

DREV R-4347/85 (UNCLASSIFIED)

Research and Development Branch, DND, Canada.
DREV, P.O. Box 8800, Courcelette, Que. GOA 1R0

"An Active Tracking Band-Pass Filter" by A. Morin and P. Labbé

A frequency-agile tracking filter, which operates over a wide frequency range with a high immunity to noise and interference, has been designed. It consists of a second-order band-pass filter which is continuously tunable over the 5- to 140-kHz band. The resonant frequency of the filter is adjusted by means of a feedback loop to the frequency component of greatest amplitude in the input signal. The loop includes a fast AGC amplifier, a fast frequency-to-voltage converter and a low-pass filter. The components of the tracking filter are described and analyzed. Analysis of the tracking filter, as regards its immunity to noise and interference, its frequency agility and the stability of its control loop, is also presented to optimize system parameters. Finally, the performance of the processor is shown by experimental measurements.

CRDV R-4347/85 (NON CLASSIFIE)

Bureau - Recherche et Développement, MDN, Canada.
CRDV, C.P. 8800, Courcelette, Qué. G0A 1R0

"Un filtre passe-bande actif de poursuite" par A. Morin et P. Labbé

On a conçu un filtre de poursuite agile en fréquence qui fonctionne dans une large bande de fréquences tout en résistant au bruit et aux interférences. Il comprend un filtre passe-bande du deuxième ordre qui est constamment accordable dans la bande de 5 à 140 kHz. Une boucle d'asservissement permet d'ajuster la fréquence du filtre à celle de la composante de fréquence ayant l'amplitude la plus élevée dans le signal d'entrée. Cette boucle comporte un amplificateur à commande automatique de gain et un convertisseur de fréquence à tension rapides ainsi qu'un filtre passe-bas. Tous les composants du filtre de poursuite sont décrits et analysés. On a aussi procédé à l'analyse du filtre de poursuite, en ce qui concerne son agilité en fréquence, sa résistance au bruit et aux interférences et la stabilité de sa boucle d'asservissement, en vue d'optimiser les paramètres du système. Finalement, la performance du filtre est démontrée par des résultats expérimentaux.

END

FILMED

8-85

DTIC